ACS APPLIED MATERIALS & INTERFACES
Letter
www.acsami.org

Effect Of Channel Layer Thickness On The Performance Of Indium−Zinc−Tin Oxide Thin Film Transistors Manufactured By Inkjet Printing

Christophe Avis, Hye Rim Hwang, and Jin Jang*

Kyung Hee University, Advanced Display Research Center and Department of Information Display, Dondaemun-gu, Seoul 130-701, Korea

ABSTRACT: We report the fabrication of high field-effect mobility of ∼110 $cm^2/(V\ s)$ for inkjet printed indium−zinc-tin oxide (IZTO) thin film transistors (TFTs). It is found that the morphology of IZTO material deposited by inkjet printing depends strongly on its thickness. When the thickness is 35 nm, IZTO is an homogeneous amorphous material and the TFT exhibits mobility over 100 $cm^2/(V\ s)$ and on/off current ratio of >10^6. However, when the thickness is 85 nm, IZTO has a two layer structure of homogeneous and heterogeneous materials and thus the TFT exhibited a mobility of ∼20 $cm^2/(V\ s)$. When the thickness is 800 nm, the morphology is porous and heterogeneous and thus the on/off current ratio is less than 1 × 10^3 and its mobility is ∼14 $cm^2/(V\ s)$. It is concluded therefore that homogeneous amorphous IZTO TFT on Al_2O_3 gate insulator can show high mobility, which can be achieved by thin layer formation by inkjet printing.

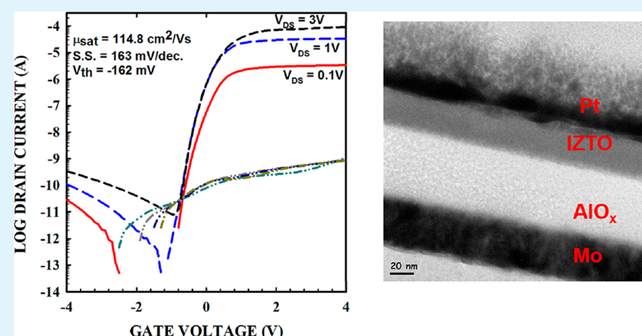

KEYWORDS: *solution processed oxides, IZTO, thin film transistors, inkjet-printing, oxide TFT, oxide semiconductor*

1. INTRODUCTION

Recently, there have been several reports on solution process techniques with a process temperature of 200−300 °C, such as hydrolysis,[1] combustion,[2] and physicochemical technique,[3] to achieve high-mobility oxide thin-film transistors (TFTs) of 1−40 $cm^2/(V\ s)$. Therefore, the performance of oxide TFT made by solution process can be as good as that of oxide TFT made by vacuum process, which was introduced by Nomura et al.[4]

The manufacturing of active-matrix liquid-crystal displays (AMLCD) and driver circuits by using solution-processed oxide TFTs has also been demonstrated.[3,5,6] Because of its simple process and low capital investment, solution processing of TFTs can be used for low-cost displays. Especially, inkjet-printing is a green technology, because the active material is deposited on demand onto the appropriate positions, without need of further etching process nor mask alignment, reducing chemicals and energy consumptions for building TFT array. On the other hand, the selection of the gate insulator[3,7,8] has been emphasized to improve TFT performances and to reduce the process temperature. Zinc−tin oxide (ZTO),[8] indium−gallium-zinc oxide (IGZO),[9] indium oxide (InO_x),[10] and indium−zinc−tin oxide (IZTO)[11] have been widely investigated as potential candidates as the active material of oxide TFTs

Spin-coated IZTO TFTs show the field-effect mobility of 90 $cm^2/(V\ s)$ when the annealing temperature was 400 °C,[11] and inkjet-printed ones exhibited the mobility of 30 $cm^2/(V\ s)$ at the process temperature of 600 °C.[12] The former reveals that by using nitrate and acetate precursors, the formation of polycrystalline phase can be seen when annealing was carried out at 400 °C. On the other hand, the latter, in which the authors use the same precursors as the present study, but with lower precursor concentration, and showed a mobility of ∼30 $cm^2/(V\ s)$ at the annealing temperature of 600 °C. The authors explained the need of a high temperature to complete the formation of the oxide network as revealed by thermogravimetric analysis (TGA) of the coated material.

The composition ratio between indium, zinc, and tin is important to achieve high mobility. By using the nitrates derivatives having Zn:Sn:In = 1:4:4, the field-effect mobility of 90 $cm^2/(V\ s)$ was achieved.[11] With chloride derivatives, the best ratio reported was Zn:Sn:In = 1:1:1,[12] exhibiting the mobility of 30 $cm^2/(V\ s)$. The difference in the IZTO layers formed by chloride or nitrate precursor could be related to the ink formulation and the chemical reactions involved in the formation of the layers.[12,13] Tin has a low solubility in indium oxide,[11] therefore a high concentration of zinc contributes to a higher solubility of tin. This leads to high mobility. as the tin s orbitals acts as the carrier pathway network, or as a carrier provider, along with the In 5s orbitals, which contributes as the electron pathway.[14] Indeed, Nomura et al.[14] reported that indium s orbitals formed the electron pathway in IGZO, and the same group also reported that in IGZO the transport phenomenon can be explained by percolation conduction

Received: February 25, 2014
Accepted: May 30, 2014
Published: May 30, 2014

 © 2014 American Chemical Society

mechanism, indicating that higher density of free carriers leads to a higher mobility.[4]

In the present work, we investigated the performance of inkjet-printed IZTO TFTs processed at the maximum temperature of 300 °C. We report the effect of layer thickness on film structure and on TFT performance using AlO_x gate insulator. Homogeneous and uniform amorphous layer can lead to mobility of >100 $cm^2/(V\ s)$, which can be achieved by using thin IZTO layer of ~35 nm. Thick IZTO has heterogeneous structure with nanopores inside and exhibits low mobility.

2. EXPERIMENTAL METHODS

2.1. Solutions fabrication. We used the chloride derivatives for the fabrication of the TFTs. Indium chloride ($InCl_3$), tin chloride ($SnCl_2$), and zinc chloride ($ZnCl_2$) were chosen as the metal precursors of indium, tin, and zinc, respectively. The amount of each precursor was scaled to be 2 m mol each and filled into a vial. Then, a 10 mL solution of acetonitrile and ethylene glycol (35 and 65% in volume, respectively) was introduced into a vial and the solution was finally stirred for 2 h. The aluminum oxide precursor solution was prepared by mixing $AlCl_3$ into a solvent of 35% acetonitrile and 65% ethylene glycol at a concentration of 0.2 M.

2.2. TFT Process. Figure 1 shows the process flow of the TFT. Mo was used as the gate electrode, the aluminum oxide precursor solution was then spin-coated as the gate insulator, then cured on a hot plate at 240 °C. Spin-coating was repeated 5 times in order to achieve 100 nm thick gate insulator. Then, indium zinc oxide (IZO) was deposited by sputtering and patterned as the source/drain electrodes. The IZTO precursor solution was inkjet-printed on the TFT backplane by using a Litrex 80.L inkjet-printer.[15] The substrate temperature was set to 25, 60, or 90 °C. The samples were then annealed at 300 °C for 2 h in air.

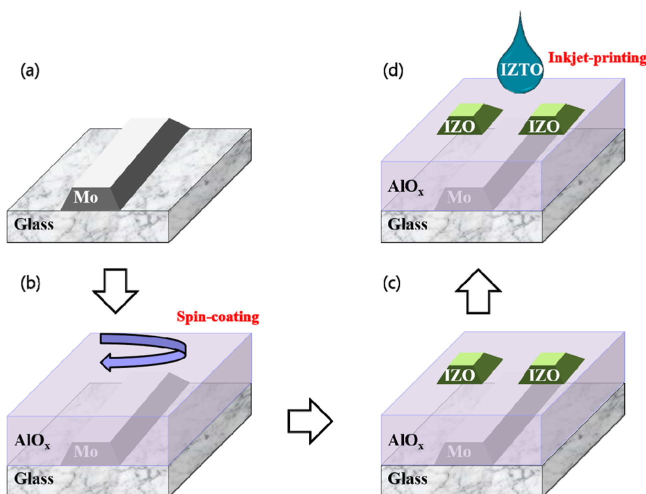

Figure 1. Process summary of solution processed oxide TFT. (a) Deposition and patterning of a 40 nm Mo gate, (b) followed by the 5 times spin-coating of the AlO_x precursor solution on the Mo gate patterned substrate, (b) evaporation of the solvent from the spin-coated AlO_x ink by hot-plate curing at 240 °C in order to obtain ~100 nm thick AlO_x. (c) Then, 40 nm of IZO was deposited and patterned as the source and drain electrodes. (d) The final step was inkjet printing of the IZTO precursor solution onto a TFT backplane. The process was carried out in air and annealed at 300 °C for 2 h in air.

2.3. Measurement. The TFTs were characterized by a precision semiconductor parameter analyzer Agilent 4156C. The field-effect mobility in the saturation region (μ_{sat}) was calculated from the square-root of drain current plot ($\sqrt{I_{DS}}$) versus gate voltage (V_{GS}) using the following equation

$$I_{DS} = \frac{C\mu_{sat}W}{2L}(V_{GS} - V_{th})^2 \quad (1)$$

where C is the capacitance of gate insulator per unit area, V_{GS} is the voltage applied between gate and source electrodes, V_{th} is the threshold voltage, W is the channel width, and L is the channel length.

3. RESULTS AND DISCUSSION

3.1. Fabrication Process. The chemical composition of AlO_x used as gate insulator is very close to Al_2O_3, with carbon content less than 5%, and chlorine below the detection limit.[8] Metal–insulator–metal (MIM) devices were used to measure its capacitance at 1 kHz and the dielectric constant from the capacitance is ~7.[8] The contact angle of water on AlO_x depends on air exposure time and the fresh AlO_x shows hydrophilic surface.[16]

3.2. TFT Performances. Figure 2 shows the summary of the TFT performances with the variation of substrate temperature during inkjet printing. The average value for the field-effect mobility of the TFTs prepared at 25, 60, and 90 °C are 44.59 ± 20, 59.24 ± 27.40, and 41.37 ± 24.96 $cm^2/(V\ s)$ and the average values of SS (subthreshold swing) are 116 ± 40, 125 ± 37, 152 ± 62 mV/dec, respectively. The average values are achieved from 14 TFTs.

Figure 3a shows the performance of a TFT exhibiting μ_{sat} of 114 $cm^2/(V\ s)$, V_{th} of −0.16 V, and SS of 163 mV/dec The ink was dropped at the center of a channel between source and drain electrodes. The coffee ring region is therefore out of the channel. Inside source/drain electrodes, the thickness of IZTO layer is ~35 nm and it has homogeneous amorphous structure without having any nanopore inside.

Figure 4a shows the transfer characteristics of an inkjet-printed TFT, with channel width of 100 μm and length of 4 μm. The thickness of oxide layer between source and drain electrodes is ~85 nm. The inset shows an optical image of the inkjet-printed channel for the corresponding TFT, exhibiting the saturation mobility of 20.4 $cm^2/(V\ s)$, V_{th} of −0.17 V, and SS of 192 mV/dec As can be seen from the optical image, the inkjet printed oxide is not centered at the TFT channel. Also, it is noticed that the drop shows the coffee ring effect, which occupies the channel region of the TFT. TEM images were taken to see the channel region of the TFT and to have an insight into the film structure. The IZTO channel layer is formed of two layers near the source/drain electrodes as shown in Figure 4b, c; ~50 nm thick porous layer on top of the AlO_x and 35 nm thick homogeneous IZTO layer. Figure 4c shows the IZTO layer in the channel region away from source/drain electrodes. Formation of porous layer by inkjet was previously reported for ZTO,[17] but not the formation of two layers. The figure reveals that near the source/drain region, the IZTO is formed of stack layers of heterogeneous and homogeneous materials. The heterogeneous layer has a lot of nanopores inside.

As shown in SEM image measured by D.-H. Lee et al.,[13] nanopores in tin oxide TFTs can be formed during the curing process of inkjet-printed oxide since the inkjet-printed layer

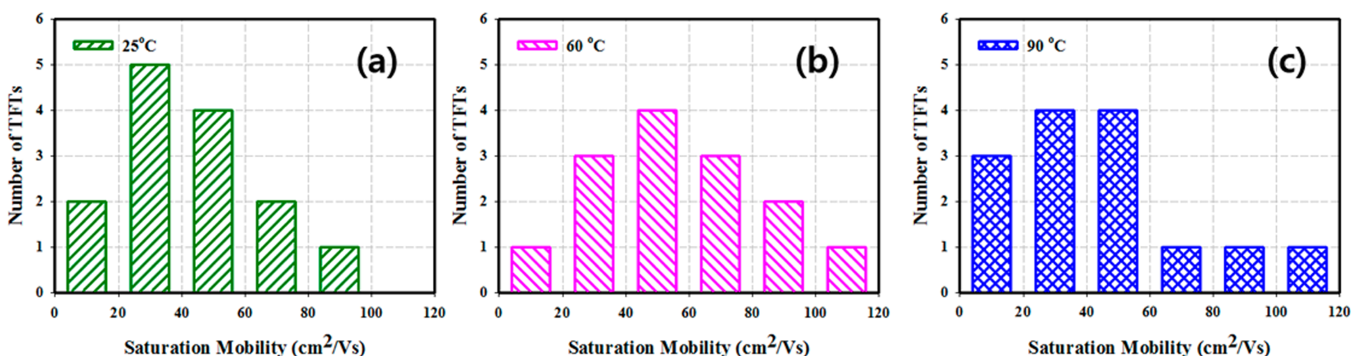

Figure 2. Comparison of the distribution of saturation mobility for 14 inkjet-printed TFTs at a substrate temperature of (a) 25, (b) 60, and (c) 90 °C. The optimal condition for inkjet printing was found to be 60 °C, where the average field-effect mobility of 60 $cm^2/(V\ s)$ was achieved. On the other hand, the TFTs processed at 25 and 90 °C had the average mobility of 43 and 35 $cm^2/(V\ s)$, respectively.

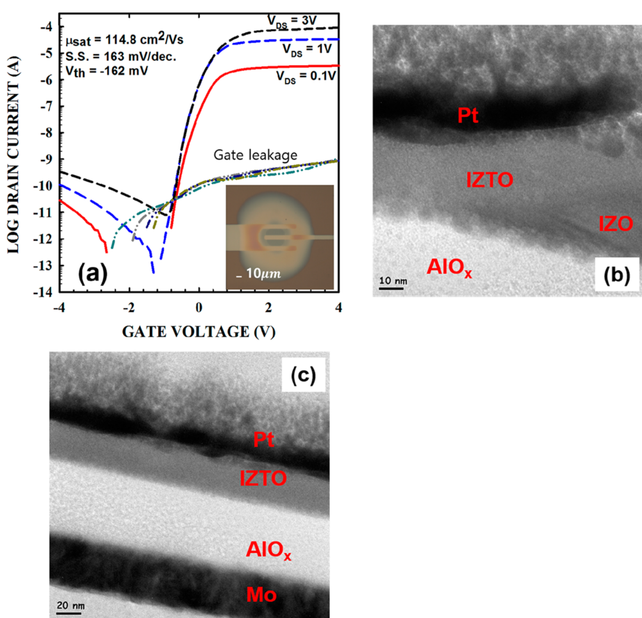

Figure 3. Performance and cross-sectional view of high-quality a-IZTO TFT. (a) Transfer curve of the inkjet-printed IZTO TFT, where saturation mobility, subthreshold slope and V_{th} were 114 $cm^2/(V\ s)$, 163 mV/dec, and −0.162 V, respectively. The figure shows the transfer curve measured at different V_{DS} of 0.1, 1, and 3 V. (b) The HRTEM image of the TFT near the IZO source/drain. The IZTO layer is uniform and homogeneous with thickness of 25−35 nm, (c) the HRTEM of the TFT in the channel layer away from the source/drain region. The IZTO layer is homogeneous and its thickness is around 35 nm. TFT W and L were 100 and 10 μm, respectively.

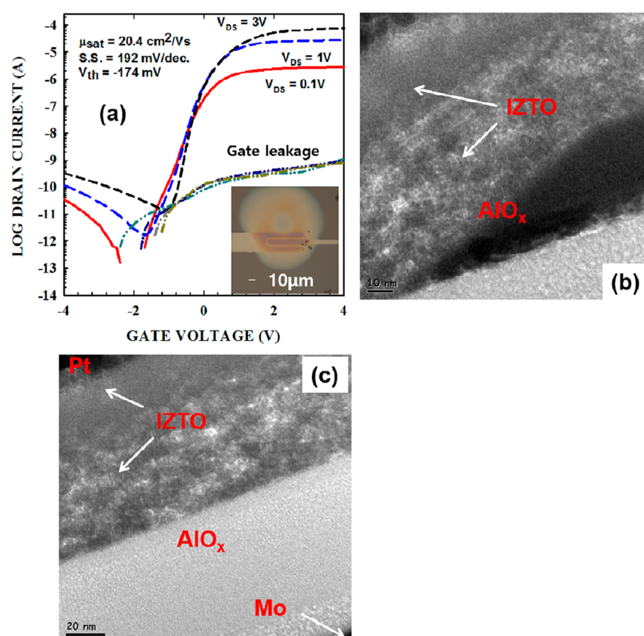

Figure 4. (a) Transfer curve of inkjet-printed IZTO TFT, where saturation mobility, subthreshold slope, and V_{th} were 20.4 $cm^2/(V\ s)$, 192 mV/dec, and −0.174 V, respectively. The figure shows the transfer curve measured at different V_{DS} of 0.1, 1, and 3 V. (b) HRTEM image of the TFT near the IZO source/drain. The IZTO has 2 sublayers, one above the AlO_x gate insulator is around 50 nm filled with nanopores, whereas the one on its top is homogeneous with ∼35 nm thickness. (c) HRTEM of the TFT in a different magnification scale. The IZTO layer in the channel can be clearly divided into 2 separated layers, one being porous, and the other one homogeneous.

reacts with H_2O in air. They suggested that the formation of HCl leads to its interaction with the layer and form bubbles in the film. The nanopores in their study have 50−200 nm width. In our case, the nanopore size does not exceed ∼30 nm.

Figure 5 shows the TFT performance with a ∼800 nm thick IZTO layer and Figure 5a shows the transfer characteristics. The TFT has a mobility of 14.1 $cm^2/(V\ s)$. Figure 5b−d show the HRTEM of the TFT channel. A bubble can be found and nanocrystal structure can be seen. The low mobility is due to the nanopores, and will be discussed further. The clear coffee ring can be seen, which is arisen by the Marangoni effect[18−21] because of the difference in surface tension between the dropped material and the surface dropped onto. The IZTO precursor solution flows away from the center leaving a thin layer in the center and rather thick layer at the edges. In the central thin layer, until a critical thickness of ∼35 nm, the IZTO precursor solution can interact with H_2O in air without perturbing its homogeneous and amorphous structure because HCl can diffuse out to the air.[22] The edge of the drop is subject to rotating convection heat, which therefore influences the interaction of HCl with its surroundings, leading to the higher probability to form nanopores because of its thick layer.

The thickness of the active material has been observed as a major parameter to affect TFT characteristics in a-Si:H,[23] IGZO TFTs made by both vacuum[24] or solution process.[25] In the case of the 800 nm thick IZTO layer, the on−off ratio is ∼1 × 10^3, induced by a high conductivity material between the source and drain electrodes.[26] As shown in Figures 3 and 4, the deterioration in the TFT performance in the thicker layer is

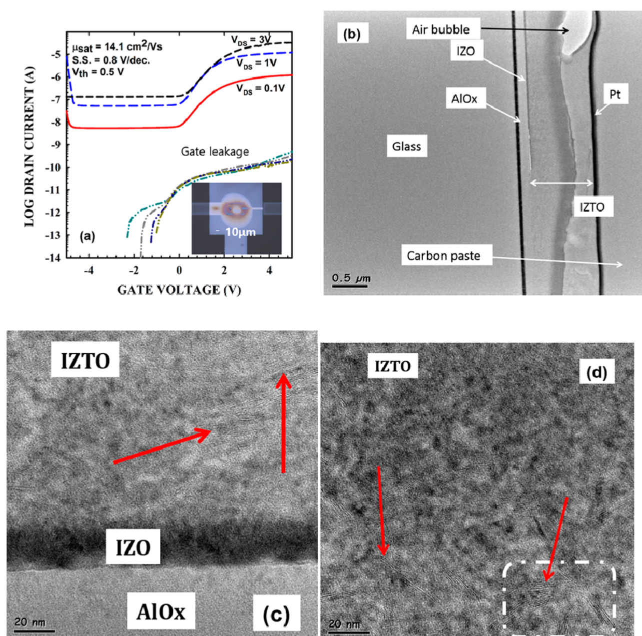

Figure 5. Performance and structure of the TFT with thick active layer and coffee-ring in a channel. (a) Transfer curve and its inset show drop shape, and (b) the TEM image of the TFT. Air bubble can be identified on the top right of the figure, which was formed during the IZTO inkjet-printing. The IZTO layer is thick and not uniform; from ~100 nm up to ~800 nm. (c) HRTEM on top of the IZO source/drain, showing nanocrystal structure. (d) Another example of the presence of nanocrystals in the IZTO layer. The red arrows in c and d indicate the location of nanocrystals.

attributed to the lower quality of material because of high density of nanopores. The SS is similar in low (~20 $cm^2/(V\ s)$) and high mobility (~100 $cm^2/(V\ s)$) TFTs. This indicates that the interface state density between the two TFTs are similar, but the density of states in the bulk appears to be very different. The degradation in performance in thick IZTO layer is also related to the high density of nanopores.

Aluminum oxide has been investigated as a gate insulator for oxide TFTs. We previously reported the use of AlO_x for ZTO TFTs and demonstrated a mobility of ~30 $cm^2/(V\ s)$.[8] Other groups exhibited high-performance TFTs through atomic layer deposition,[27] or anodic deposition of AlO_x.[28] The reason for the improved performance has been ascribed to the high conduction band offset,[29] lowering of the source drain contact resistance and the lowering of the channel resistance.[26] It was also proposed that Al can diffuse into the channel leading to the increase of mobility.[30]

4. CONCLUSIONS

We have studied the effect of IZTO thickness on the performance of inkjet printed TFTs on AlO_x gate insulator. Field-effect mobility of ~110 $cm^2/(V\ s)$ was achieved by using 35 nm thick IZTO layer which has homogeneous and amorphous structure. On the other hand, 85 nm thick IZTO has two layer structure of homogeneous and heterogeneous materials and thus exhibited mobility of ~20 $cm^2/(V\ s)$. The 800 nm thick IZTO layer has a lot of nanopores inside and thus exhibited very high off-state currents and saturation mobility of ~14 $cm^2/(V\ s)$. It is also found that AlO_x is important in achieving high-performance TFT because it helps IZTO to have a higher density of oxygen−metal bonds compared to the IZTO on SiO_2.

■ AUTHOR INFORMATION

Corresponding Author

*E-mail: jjang@khu.ac.kr. Tel: +82-2-961-0688. Fax: +82-2-961-9154.

Notes

The authors declare no competing financial interest.

■ ACKNOWLEDGMENTS

This work was supported by the Industrial Strategic Technology Development Program (10045269, Development of Soluble TFT and Pixel Formation Materials/Process Technologies for AMOLED TV) funded by MOTIE/KEIT.

■ REFERENCES

(1) Banger, K. K.; Yamashita, Y.; Mori, K.; Peterson, R. L.; Leedham, T.; Rickard, J.; Sirringhaus, H. Low-temperature, high-performance solution-processed metal oxide thin-film transistors formed by a "sol−gel on chip" process. *Nat. Mater.* **2011**, *10*, 45−50.

(2) Kim, Y.-H.; Heo, J.-S.; Kim, T.-H.; Park, S.; Yoon, M.-H.; Kim, J.; Oh, M. S.; Yi, G.-R.; Noh, Y.-Y.; Park, S. K. Flexible metal-oxide devices made by room-temperature photochemical activation of sol−gel films. *Nature* **2012**, *489*, 128−132.

(3) Kim, M.-G.; Kanatzidis, M. G.; Facchetti, A.; Marks, T. J. Low-temperature fabrication of high-performance metal oxide thin-film electronics via combustion processing. *Nat. Mater.* **2011**, *10*, 382−388.

(4) Nomura, K.; Ohta, H.; Takagi, A.; Kamiya, T.; Hirano, M.; Hosono, H. Room-temperature fabrication of transparent flexible thin-film transistors using amorphous oxide semiconductors. *Nature.* **2004**, *432*, 488−492.

(5) Kim, B. S.; Jeong, Y. T.; Lee, D.; Choi, T.; Jung, S.-H.; Choi, J. W.; Yang, C.; Jo, K.; Lee, B.-J.; Park, E.; Kim, D. N.; Kim, Y.; Shin, S. Solution-processed zinc-indium-tin oxide thin-film transistors for flat-panel displays. *Appl. Phys. Lett.* **2013**, *103*, 072110.

(6) Kim, Y.-H.; Kim, K.-H.; Oh, M. S.; Kim, H. J.; Han, J. I.; Han, M.-K.; Park, S. K. Ink-jet-printed zinc−tin−oxide thin-film transistors and circuits with rapid thermal annealing process. *IEEE Eletron Device Lett.* **2010**, *31*, 836−838.

(7) Pal, B. N.; Dhar, B. M.; See, K. C.; Katz, H. E. Solution-deposited sodium beta-alumina gate dielectrics for low-voltage and transparent field-effect transistors. *Nat. Mater.* **2009**, *8*, 898−903.

(8) Avis, C.; Jang, J. High-performance solution processed oxide TFT with aluminum oxide gate dielectric fabricated by a sol−gel method. *J. Mater. Chem.* **2011**, *21*, 10649−10652.

(9) Wang, Y.; Sun, X. W.; Goh, G. K. L.; Demir, H. V.; Yu, H. Y. Influence of Channel Layer Thickness on the Electrical Performances of Inkjet-Printed In-Ga-Zn Oxide Thin-Film Transistors. *IEEE Trans. Electron Devices* **2011**, *58*, 480−485.

(10) Han, S.-Y.; Herman, G. S.; Chang, C.-H. Low-temperature, high-performance, solution-processed indium oxide thin-film transistors. *J. Am. Chem. Soc.* **2011**, *133*, 5166−5169.

(11) Kim, M.-G.; Kim, H. S.; Ha, Y.-G.; He, J.; Kanatzidis, M.; Facchetti, A.; Marks, T. High-performance solution-processed amorphous zinc-indium-tin oxide thin-film transistors. *J. Am. Chem. Soc.* **2010**, *132*, 10352−10364.

(12) Lee, D.-H.; Han, S.-Y.; Herman, G. S.; Chang, C.-H. Inkjet printed high-mobility indium zinc tin oxide thin film transistors. *J. Mater. Chem.* **2009**, *20*, 3135−3137.

(13) Lee, D.-H.; Chang, Y.-J.; Stickle, W.; Chang, C.-H. Functional Porous Tin Oxide Thin Films Fabricated by Inkjet Printing Process. *Electrochem. Solid-State Lett.* **2007**, *10*, K51−K54.

(14) Nomura, K.; Kamiya, T.; Ohta, H.; Uruga, T.; Hirano, M.; Hosono, H. Local coordination structure and electronic structure of the large electron mobility amorphous oxide semiconductor In-Ga-Zn-

O: Experiment and *ab initio* calculations. *Phys. Rev. B: Condens. Matter Mater. Phys.* **2007**, *75*, 035212−5.
(15) Kim, C. H.; Choi, M. H.; Lee, S. H.; Jang, J.; Kirchmeyer, S. Dependence of persistent photocurrent on gate bias in inkjet printed organic thin-film transistor. *Appl. Phys. Lett.* **2010**, *96*, 123301.
(16) Choi, J.-M.; Hwang, D. K.; Jeong, S. H.; Park, J. H.; Kim, E.; Kim, J. H.; Im, S. Polymer/ AlO_x Bilayer Dielectrics for Low-Voltage Organic Thin-Film Transistors. *J. Electrochem. Soc.* **2007**, *154*, H331−H335.
(17) Jeong, Y.; Song, K.; Kim, D.; Koo, C. Y.; Moon, J. Bias Stress Stability of Solution-Processed Zinc Tin Oxide Thin-Film Transistors. *J. Electrochem. Soc.* **2009**, *156*, H808−H812.
(18) Hu, H.; Larson, R. G. Marangoni Effect Reverses Coffee-Ring Depositions. *J. Phys. Chem. B* **2006**, *110*, 7090−7094.
(19) Lim, J. A.; Lee, W. H.; Lee, H. S.; Lee, J. H.; Park, Y. D.; Cho, K. Self-Organization of Ink-jet-Printed Triisopropylsilylethynyl Pentacene via Evaporation-Induced Flows in a Drying Droplet. *Adv. Funct. Mater.* **2008**, *18*, 229−234.
(20) Kim, Y.-H.; Kim, K.-H.; Oh, M. S.; Kim, H. J.; Han, J. I.; Han, M.-K.; Park, S. K. Ink-Jet-Printed Zinc−Tin−Oxide Thin-Film Transistors and Circuits With Rapid Thermal Annealing Process. *IEEE Electron Device Lett.* **2010**, *31*, 836−838.
(21) De Gans, B.-J.; Duineveld, P. C.; Schubert, U. S. Polymer-Relief Microstructures by Inkjet Etching. *Adv. Mater.* **2004**, *16*, 203−213.
(22) Lee, D. H.; Chang, Y.-J.; Herman, G. S.; Chang, C.-H. A General Route to Printable High-Mobility Transparent Amorphous Oxide Semiconductors. *Adv. Mater.* **2007**, *19*, 843−847.
(23) Martin, S.; Chiang, C.-S.; Nahm, J.-Y.; Kanicki, J.; Ugai, Y. Influence of the Amorphous Silicon Thickness on Top Gate Thin-Film Transistor Electrical Performances. *Jpn. J. Appl. Phys.* **2001**, *40*, 530−537.
(24) Barquinha, P.; Pereira, L.; Goncalves, C.; Martins, R.; Fortunato, E. Toward High-Performance Amorphous GIZO TFTs. *J. Electrochem. Soc.* **2009**, *156*, H161−H168.
(25) Wang, Y.; Sun, X. W.; Goh, G. K. L.; Demir, H. V.; Yu, H. Y. Influence of Channel Layer Thickness on the Electrical Performances of Inkjet-Printed In-Ga-Zn Oxide Thin-Film Transistors. *IEEE Trans. Electron Devices* **2011**, *58*, 480−485.
(26) Kim, D.; Jeong, Y.; Koo, C. Y.; Song, K.; Moon, J. Thin Film Transistors with Ink-Jet Printed Amorphous Oxide Semiconductors. *Jpn. J. Appl. Phys.* **2010**, *49*, 05EB06−4.
(27) Woo, C. H.; Ahn, C. H.; Kwon, Y. H.; Lee, J.-H.; Cho, H. K. Transparent and flexible oxide thin-film-transistors using an aluminum oxide gate insulator grown at low temperature by atomic layer deposition. *Metals Mater. Int.* **2012**, *18*, 1055−1060.
(28) Lan, L.; Peng, J. High-Performance Indium−Gallium−Zinc Oxide Thin-Film Transistors Based on Anodic Aluminum Oxide. *IEEE Trans. Electron Devices* **2011**, *58*, 1452−1455.
(29) Cho, H.; Douglas, E. A.; Scheurmann, A.; Gila, B. P.; Craciun, V.; Lambers, E. S.; Pearton, S. J.; Ren, F. $Al_2O_3/InGaZnO_4$ Heterojunction Band Offsets by X-Ray Photoelectron Spectroscopy. *Electrochem Solid-State Lett.* **2011**, *11*, H431−H433.
(30) Nayak, P. K.; Hedhili, M. N.; Cha, D.; Alshareef, H. N. High performance In_2O_3 thin film transistors using chemically derived aluminum oxide dielectric. *Appl. Phys. Lett.* **2013**, *103*, 033518.